International Journal of Engineering and Geosciences
https://dergipark.org.tr/en/pub/ijeg
e-ISSN 2548-0960

Evaluation of the Origin and Synoptic Analysis of Dust Storm Phenomena Using Satellite Image Processing in Western Iran

Ali Ibrahim Zaghir [1], Khalil Valizadeh Kamran [*1], Sadra Karimzadeh [1]

[1] *University of Tabriz, Department of Remote sensing and GIS, Iran, khvaka@yahoo.com,valizadeh@tabrizu.ac.ir, sa.karimzadeh@ tabrizu.ac.ir*

Cite this study: Zaghir, A.I.,Kamran, K. V., & Karimzadeh, S., (2025). Evaluation of the Origin and Synoptic Analysis of Dust Storm Phenomena Using Satellite Image Processing in Western Iran. International Journal of Engineering and Geosciences, 10(3), 419-427

https://doi.org/10.26833/ijeg.1576113

Keywords
Dust storms,
MODIS sensors,
Terra and Aqua,
Monitoring and synoptic analysis

Research Article

Received:31.10.2024
Revised: 01.03.2025
Accepted:17.03.2025
Published:01.10.2025

Abstract

This study investigates the identification and analysis of dust sources using satellite imagery and synoptic meteorological data, focusing on a significant dust event originating from Syria on September 1, 2015. Visual interpretation of satellite images, complemented by the Brightness Temperature Difference (BTD) index, confirmed the accuracy of dust source identification. The analysis revealed that an active low-pressure system in the eastern Mediterranean facilitated dust formation due to low humidity conditions. Dust movement was predominantly directed from northwest to southeast, impacting regions in southwestern Iran, including Kermanshah, Ilam, and Khuzestan. Additionally, the study examined wind patterns, demonstrating how zonal and meridional winds contributed to dust transport and dissipation. A comparative analysis of vegetation cover over a decade indicated a significant decline at the dust formation site, suggesting a correlation between reduced vegetation and increased dust emissions. This research underscores the complex interplay between atmospheric dynamics and regional environmental changes, highlighting the need for further investigation into the long-term impacts of vegetation loss on dust storm frequency and intensity. The findings aim to enhance our understanding of dust storm mechanisms and inform strategies for mitigating their adverse effects on human health and the environme.

1. Introduction

The close relationship between climate and human health and activities necessitates the study and observation of atmospheric events [1]. Dust, recognized as one of the most important atmospheric phenomena and natural disasters, has attracted the attention of many scholars and researchers in various scientific fields, including water engineering sciences. The origin and mechanism of formation, transfer, dispersion, and consequences of this phenomenon are studied using various techniques and methods. Countries located in the world's arid and semi-arid belt, including Iran, have always been dealing with dust phenomena. The occurrence of frequent droughts in recent years and the potential consequences of climate change regarding desertification have now placed dust storms at the center of attention for many researchers. The frequency of dust storms in arid and semi-arid regions is much higher and has significantly affected living conditions in many countries in the arid and semi-arid regions of Asia [2].This phenomenon is shaped by natural and human factors. Human changes in the natural environment are a very important factor in increasing the concern of some dust source areas [2]

Zolfaghari (2005) examined dust systems in western Iran with a synoptic approach over a 5-year period. He states that the Azores high pressure along with western migrant systems are the most important synoptic factors affecting dust systems. He also considers the Syrian desert, the Nafud desert in northern Arabian

Peninsula, and the northern Sahara Desert as the most important sources of dust entering western Iran. [3]

Raeispour, (2008) Statistical analysis of the dust phenomenon in Khuzestan province over a ten-year period from 1996 to 2005 shows that the average number of dusty days in the warm period of the year is higher than in the cold period, with spring having the highest number of dusty days and autumn having the lowest. [4]

Maghrabi et al. (2011), using meteorological and satellite parameters, concluded that air pressure and relative humidity increase on the day of dust occurrence compared to the previous day, while visibility and temperature decrease. Explaining how dust storms occur seems impossible without considering atmospheric circulation patterns. [5,24,25]

The aim of the research is to identify the origin of the dust on September 1, 2015, which, using MODIS satellite images and synoptic analysis of dusty days, points to the factors causing this phenomenon.

2. Method

2.1 . the Study Area

. The study are awas syria which is located in southwestern Asia, along the Mediterranean Sea, bordering Turkey to the north, Iraq to the east and southeast, Jordan to the south, Palestine to the southwest, and Lebanon to the west (Figure 1). Its climate is temperate and humid (Mediterranean) in the coastal and southwestern regions, and hot and dry in other areas. The highest point from sea level is Mount Hermon at 2,814 meters. Important rivers include the Euphrates, Khabur, Orontes, Afrin, Qoueiq, and Tigris, with the Euphrates being the longest at 2,696 kilometers, about half of which flows through Turkey and Iraq.

2-2. Climate and Precipitation of the Study Area

Syria is influenced by a Mediterranean climate. Annual rainfall ranges from about 300 to 500 mm in the coastal area, about 200 mm more in the Damascus valley interior, and 127 mm to less than 25 mm in the desert area in the southeast.

2-3. Data Used

The data and information used in this research include four series of information:

Remote sensing data, including MODIS sensor images from Terra and Aqua satellites related to the dust phenomenon from August 31, 2015 to September 2, 2015, including the bands used in the research, which were obtained from ladsweb.modaps.eosdis.nasa.gov. Also, geopotential height data for 500 mb pressure level (HGT) as well as zonal and meridional wind data (u and v components) for 1000 mb and 500 mb pressure levels related to the dust event were used. These data were obtained from the NCEP/NCAR database of the U.S. National Oceanic and Atmospheric Administration. Then, images related to the vegetation cover status of the region over a 10-year period from 2005 to 2015 were obtained from glam1.gsfc.nasa.gov and analyzed.

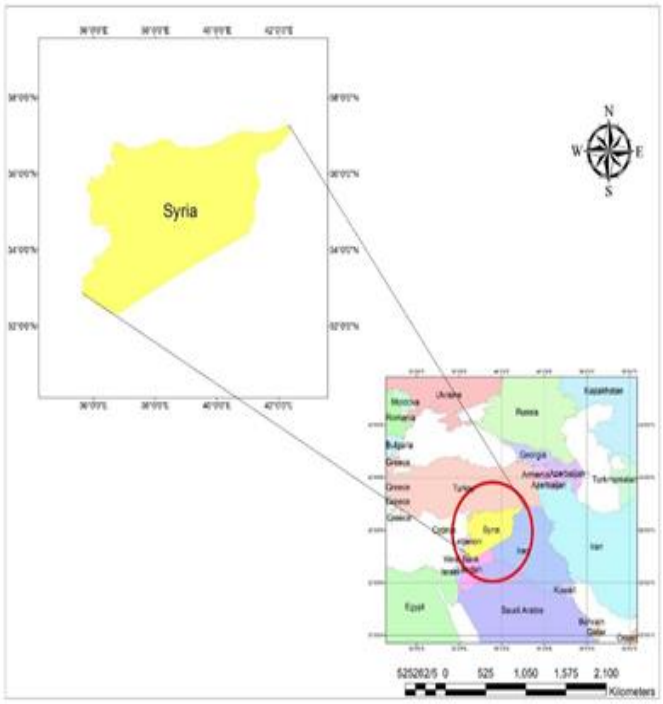

Figure 1. Map of the study area

Pre-processing: Considering that satellite images are always susceptible to various systematic and non-systematic errors from the perspective of spatial, temporal, and spectral resolutions, initial processing must be performed on raw data to correct any common errors and distortions through the imaging system or atmospheric conditions at the time of sensing.

- **Geometric Correction**

Satellite images usually have deviations that make them incompatible with maps. These deviations typically occur due to changes in longitude, sensor platform status and speed, Earth's curvature, displacement and non-linearity of movement path, sensor's instantaneous field of view, and atmospheric refractions.

In the geometric correction process, two types of corrections are applied:

a) Systematic correction, which is applied before the images are made available to users due to constant changes.

b) Non-systematic correction, which must be applied before using the images.

The images used in this research were obtained through NASA's website and then geometrically corrected using ENVI software.

- **Atmospheric Correction**

Electromagnetic energy detected by remote sensing (especially the part of the spectrum that operates in the optical region) includes a combination of energy scattered by the atmosphere. The intensity and volume of electromagnetic energy emitted in the visible and near-infrared spectral regions that reach the sensor above the atmosphere depend on the intensity of solar energy, which is attenuated by the atmospheric absorption process and surface reflectance characteristics. Therefore, the energy received by the sensor is a function of Incident energy, Feature reflectance capability, Atmospheric scattered energy and Atmospheric absorption rate

Based on this, it can be said that the numerical value of each pixel in remote sensing images is not an actual record of the Earth's surface radiance. This is because signals are attenuated due to absorption, or their path changes due to scattering. Atmospheric effects for remote sensing images are determined according to the geographical location and time of imaging. Given that clouds affect the pixel values of their adjacent areas and cause image darkening, to remove these effects from the images, a general method based on reducing the darkness of dark pixel numerical values in ENVI software was used. This method has high accuracy in atmospheric correction and is widely used in research.

When a dust storm occurs, a large amount of dust particles forms a layer. This thick dust layer can absorb and reflect solar radiation. Among the 39 MODIS bands, visible and near-infrared bands are used to measure reflection, and thermal infrared bands are used to measure the brightness temperature of objects. By comparing spectral characteristics among dust, land, and clouds, it can be found that clouds have high reflection but low brightness temperature, land has low reflection but high brightness temperature, and dust is between these two phenomena [6].

The negative and positive DNs of the dust phenomenon are related to the difference in radiative temperature above the dust phenomenon compared to other phenomena in band 32 relative to band 31(Equation 1) [6].

BTD = B31 - B32 (Equation 1)

In another method, a false color composite of bands 3, 1, and 4 [6]. was used to visually distinguish the dust phenomenon from other phenomena. R(3)G(1)B(4).

Synoptic data related to the dust day were obtained from the U.S. National Oceanic and Atmospheric Administration website and analyzed.

Then, vegetation cover status images were obtained from glam1.gsfc.nasa.gov and examined.

1.1. NDDI Index:

The NDDI index is based on the difference between spectral ranges with wavelengths of 2.13 and 0.469 micrometers. This index has advantages because it has high sensitivity in the 2.1 micrometer MODIS band to moisture content(Equation 2). [6,23].

NDDI = (b1 –b2) / (b1+b2) (Equation 2).

Where b1 and b2 are MODIS bands 7 and 3, respectively. Figure 2 shows the index image.

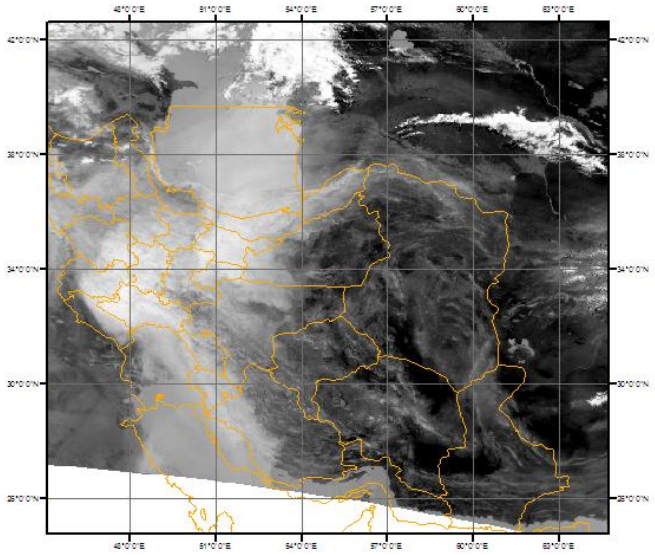

Figure 2 shows the result of applying this index to the relevant image.

1.2. BTDI (Brightness Temperature Difference Index):

The Brightness Temperature Difference Index (BTDI) can detect dust storms and dust and sand concentration using two spectral bands. The BTDI index is related to the particle size of sand and dust [7].For this index, MODIS bands 31 and 32 (thermal bands) are used. In the thermal band range, absorption by other atmospheric gases is less. In bands 31 and 32, the difference in radiation between land and dust is very high, meaning dust has higher radiation in band 31 compared to band 32 (Equation3).

BTDI = b1-b2 (Equation3)

Where b1 and b2 are thermal bands 31 and 32.

Figure 3 shows the index image.

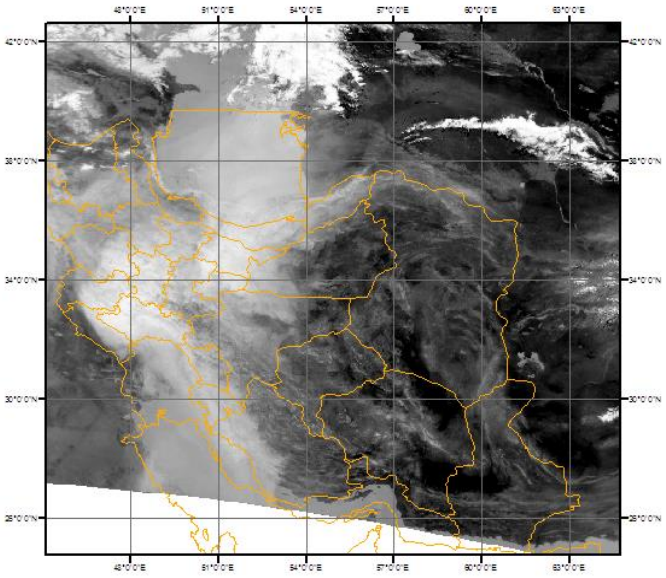

Figure 3. shows the result of applying the BTDI index to the image.

1.3. LBTDI Index:

On the other hand, MODIS reflective bands, namely band 1, show high reflection for clouds, low reflection for land, and medium reflection for dust. Also, MODIS band 3 has a high value for clouds. In fact, using thermal bands (31 and 32) and reflective bands (1 and 3), an index can be created to distinguish clouds from dust[7](Equation 4).

LBTDI = (b3+b1) + b32-b31 (Equation 4).

Figure 4 shows the index image

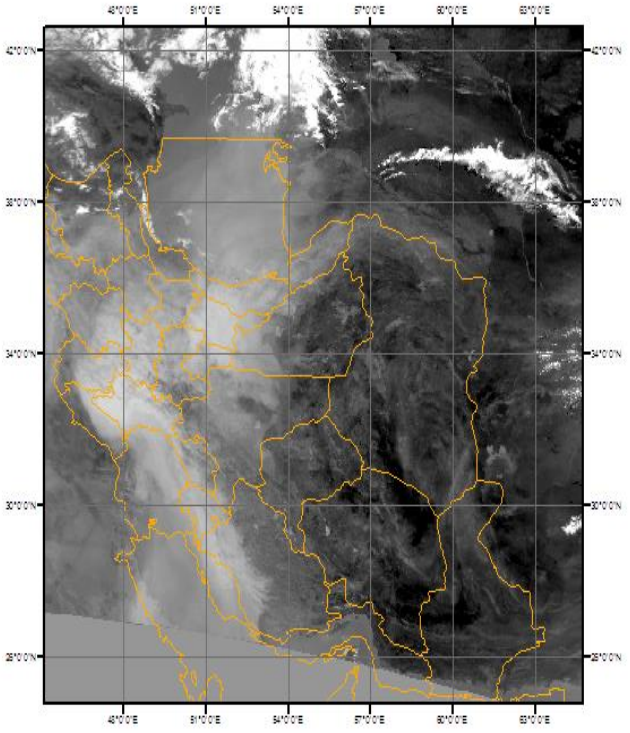

Figure 4 shows the result of applying the LBTDI index to the relevant image.

1.4. Comparison of Indices:

The results of the NDDI index on the study area show that the numerical values for clouds and water are less than zero, which is due to higher reflection of clouds and water in band 3 compared to band 7. In this index, the numerical values of land and dust fall within the same range, therefore this index does not have the power to distinguish the dust phenomenon from land.

The Brightness Temperature Difference Index (BTDI) is the result of the difference between thermal bands 32 and 31. Thermal band 32 has low radiation and temperature in clouds and very high radiation and temperature on land, with dust radiation falling between these two phenomena. Band 31 is similar to band 32, with the difference that in band 31, the radiation levels of phenomena are higher than in band 32. Subtracting band 32 from band 31 results in negative radiation for all phenomena. In this index, land and dust are easily distinguished from each other, but dust and clouds cannot be differentiated, and areas with numerical values of dense dust are observed on clouds. This index produces very favorable results in cloud-free areas. The reason for the lack of distinction between clouds and dust in this index is the presence of less dense clouds around voluminous clouds, which cause numerical values equal to areas with dense dust.

The opposite is true for the BTD index, where the obtained numerical values show that dust shares common numerical values with some parts of clouds, causing uncertainty in dust detection.

The LBTDI index is a modified version of the BTDI index. Since in the BTDI index, parts of clouds and dust have the same numerical values, bands 1 and 3 are combined due to their high cloud reflection in the MODIS sensor to increase cloud reflection. This index has better power to distinguish dust from other phenomena.

The false color composite resulting from bands 1 (red), 3 (green), and 4 (blue) visually shows a better result for observing dust in Iran on MODIS satellite images. This is due to the higher reflection of clouds in all three bands compared to land, with dust reflection falling between them.

3. Results

3.1 Dust Source mapping Using Satellite Images

In this research, first, visual interpretation was used to determine the time of dust formation and its movement using satellite images. Then, the BTD index was applied to the dust on September 1, confirming the accuracy of the work. Subsequently, by interpreting satellite images, the location of dust formation was identified as Syria, which is one of the dust occurrence sites.(Figures 5,6,7,8) Below are satellite images related to dust, observed with the band combination: R(3)G(1)B(4), used for visual interpretation.

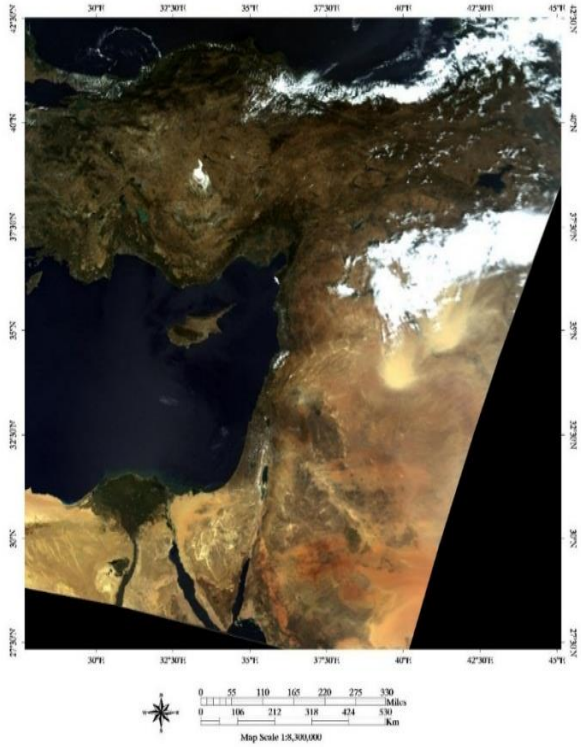

Figure 5. Image date:; August 31, 2015, 08:50

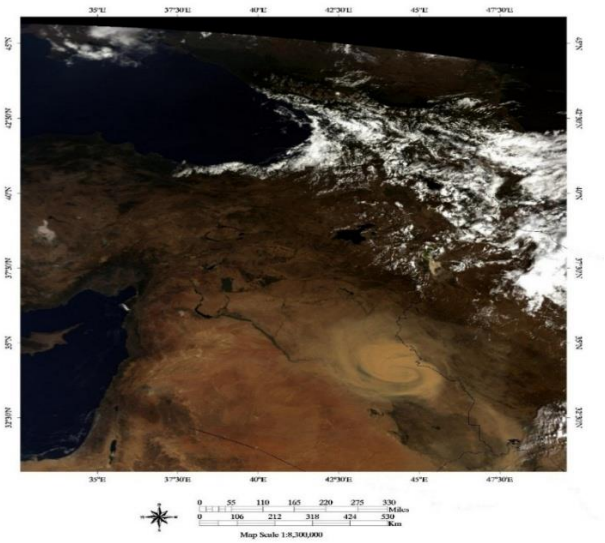

Figure 6. Image date: September 1, 2015, 07:55

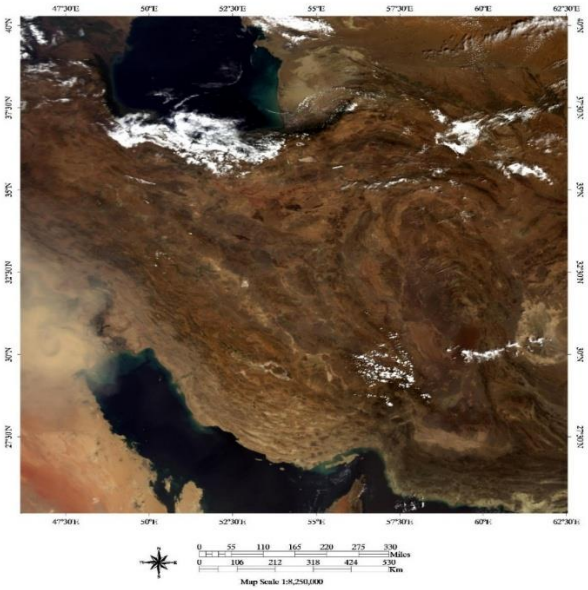

Figure 7. Image date:; September 2, 2015, 07:00

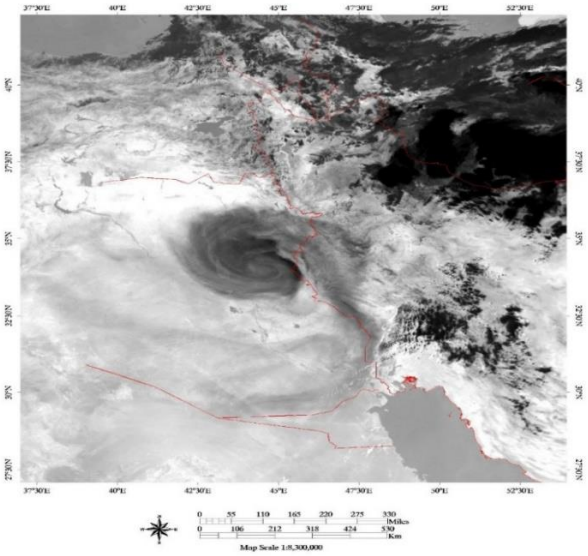

Figure 8. BTD index image of the dust day, September 1, 2015

4.2. Analysis and Interpretation of Synoptic Dust Data

The dust originated from the eastern Mediterranean region, specifically Syria. The cause of its formation is an active low-pressure system located in the eastern Mediterranean. Systems moving from the Mediterranean towards our country, intended for rainfall, cause dust due to the low humidity in the region. The source of this dust is from the eastern Mediterranean, reaching Iran's borders. Depending on particle size, it can advance to central Iran - smaller particles can travel further distances. While monitoring satellite images, the dust movement direction is northwest to southeast. The sources of dust affecting Iran are formed in Saudi Arabia, Iraq, and eastern Syria. The source of the cyclone that is active and causes precipitation is the Mediterranean Sea. Since the winds are westerly in Iran, this dust often covers Kermanshah, Ilam, and Khuzestan. [15], [16]

In a region, depending on its position relative to the equator (near, far, or in the north or south), a cyclone creates instability. In seas and oceans, tropical cyclones create storms that cause monsoon rains in our southeast, but we don't have monsoon rains in western Iran. In the west, if we have humidity and vorticity, we would have monsoon rains, but we have an enhancer from the Mediterranean that sends a vortex. Given that Iraq, Syria, and Saudi Arabia lack sufficient humidity, it mostly causes dust.

The source of dust in western Iran is extra-regional, but there is an exception - we also have an intra-regional source in Khuzestan province that intensifies dust in western Iran. On the other hand, we have internal dust sources in eastern Iran due to deserts and winds, but these dust sources cannot enter central Iran because our currents are westerly, so they remain in the eastern border areas, causing problems for those regions.

The figure 8 shows the dust on September 1, 2015, with numbers between 2205 and 2190, indicating a low-pressure cyclone rotating counterclockwise. (Figure 9)

U wind (zonal wind): This wind blows from west to east, demonstrating the alignment of common synoptic features in satellite images. The cyclone in the eastern Mediterranean has gradually extended to southwestern Iran. Wind intensity is related to the contours in the figure - the closer the contours, the stronger the wind. As it extends to southwestern Iran, dust is repelled due to the water vapor from the Persian Gulf, which can be verified by observing the increasing distance between contours. (Figure 10)

V wind (meridional): It shows that a low-pressure cyclone dominates the dust area. Both easterly and northerly winds, and the dust formed from the eastern Mediterranean extending to the southwest, are dominant. Eventually, as the contours separate, its power diminishes. (Figure 11)

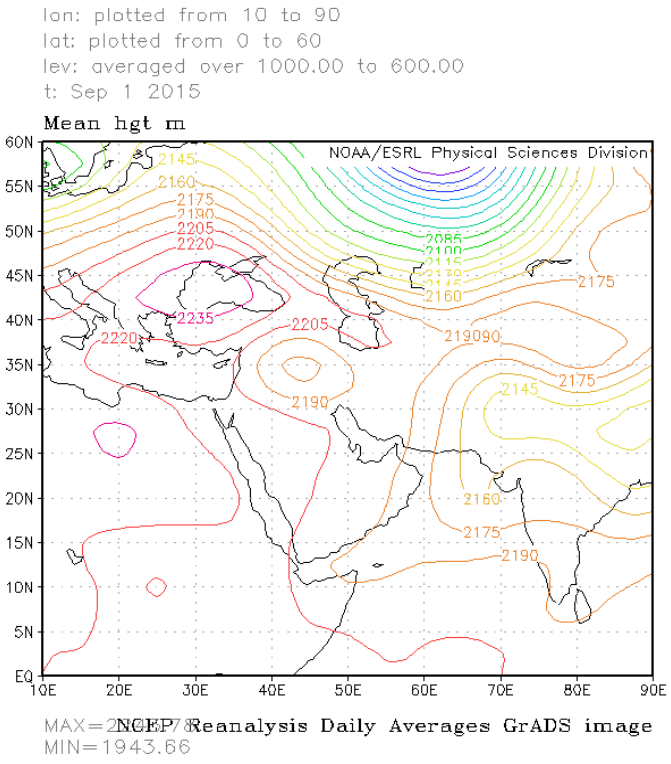

Figure 9. Geopotential height map; September 1, 2015

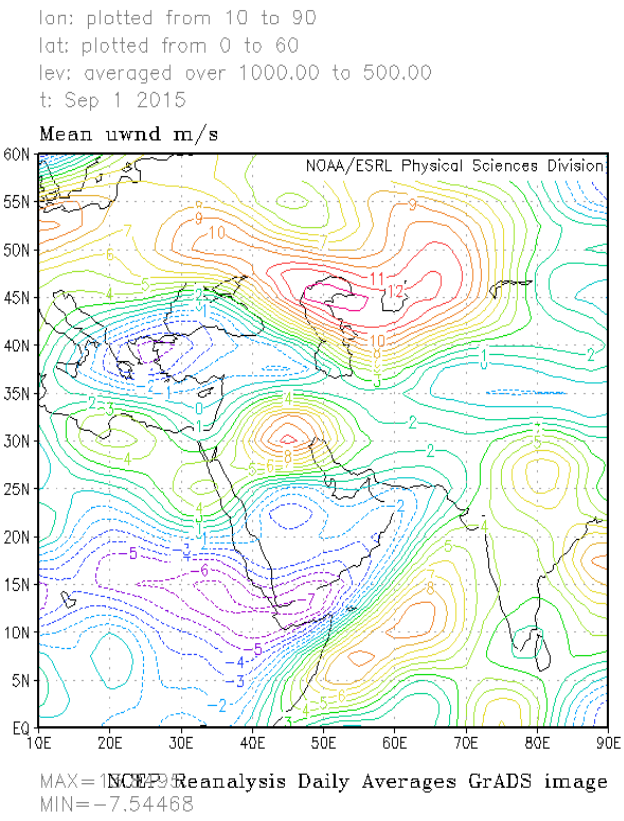

Figure 10. Zonal wind map; September 1, 2015

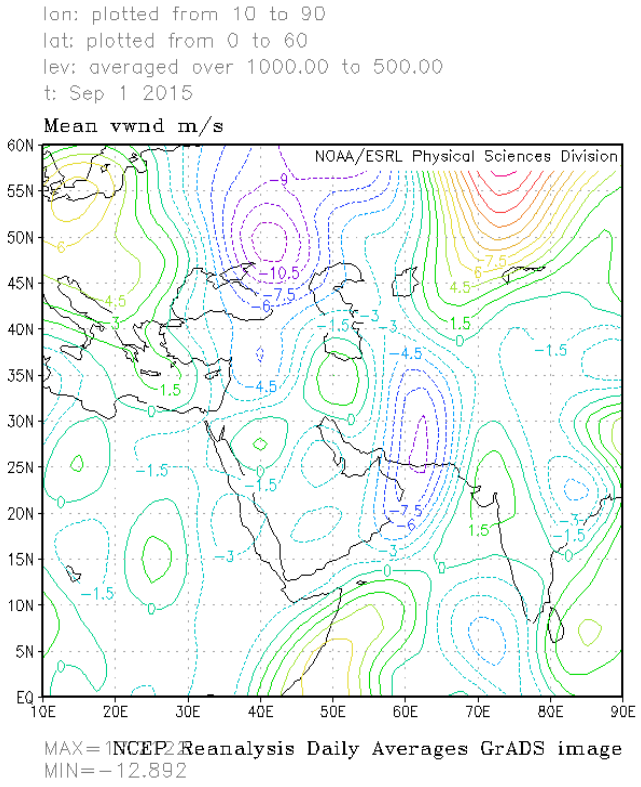

Figure 11. Meridional wind map; September 1, 2015

5.3. Examining the vegetation cover status of the study area

The vegetation cover was examined over a 10-year period, and we observed a decrease in vegetation cover at the dust formation site, which can be seen in Figures 12 and 13.

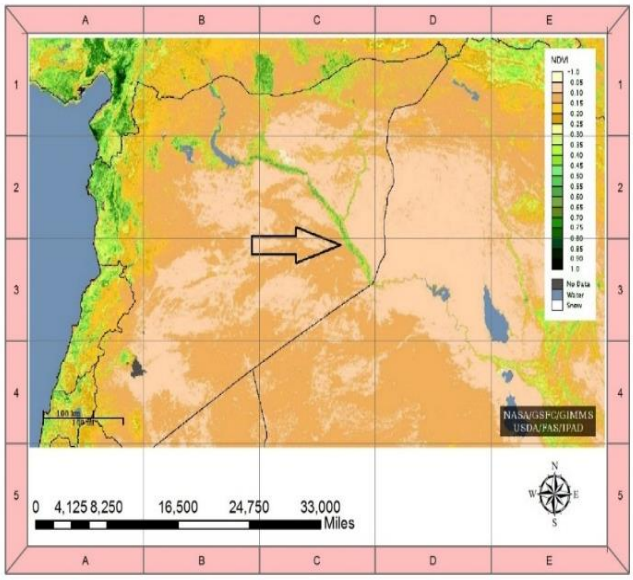

Figure 12. Vegetation cover status map on September 1, 2005

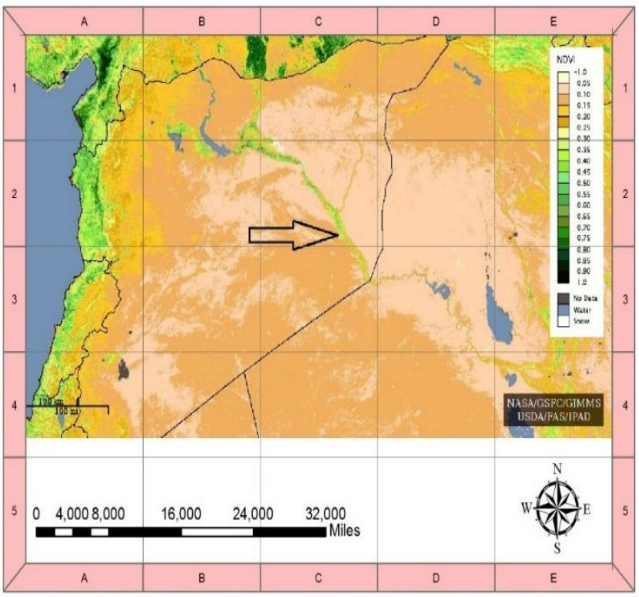

Figure 13. Vegetation cover status map on September 1, 2015

4. Discussion

4.1 Dust Source Identification and Analysis

4.1.1 Satellite Imagery Interpretation

Visual interpretation of satellite images proved effective in identifying the dust formation time and movement patterns[8][9]. The BTD index applied on September 1 confirmed the accuracy of the visual analysis, pinpointing Syria as the primary dust source location[10]. This aligns with previous studies that have identified Syria as a significant dust emission source in the region[11,22].

4.1.2 Synoptic Analysis

The dust event originated from a low-pressure system in the eastern Mediterranean, specifically over Syria[12]. This system, typically associated with rainfall, instead generated dust due to the region's low humidity. The dust movement followed a northwest to southeast trajectory, affecting areas including Kermanshah, Ilam, and Khuzestan in Iran[13].

4.2 Cyclonic Activity and Dust Generation

The position of the cyclone relative to the equator plays a crucial role in creating instability and dust generation[14]. In this case, the lack of sufficient humidity in Iraq, Syria, and Saudi Arabia resulted in dust formation rather than precipitation. This highlights the complex interplay between atmospheric conditions and regional geography in dust storm development.

4.3 Wind Patterns and Dust Transport

Analysis of zonal (U) and meridional (V) winds provided insights into the dust transport mechanisms:

- The zonal wind showed the extension of the cyclone from the eastern Mediterranean to southwestern Iran.
- The meridional wind analysis confirmed the dominance of a low-pressure system in the dust-affected area.

These wind patterns explain the observed dust movement and its eventual dissipation as it approached the Persian Gulf region.

4.4 Vegetation Cover Analysis

A 10-year comparison of vegetation cover in the study area revealed a significant decrease at the dust formation site. This reduction in vegetation likely contributed to increased dust emissions, as bare soil is more susceptible to wind erosion. The observed vegetation loss may be attributed to factors such as climate change, land use changes, or conflict-related environmental degradation in Syria. [17], [18]

4.5 Implications and Future Research

This study demonstrates the value of integrating satellite imagery, meteorological data, and vegetation analysis in understanding dust storm dynamics. Future research should focus on:

- Quantifying the relationship between vegetation loss and dust emission rates in the region.
- Investigating the long-term impacts of geopolitical events on land cover changes and subsequent dust storm frequency.
- Developing improved early warning systems for dust storms based on the identified formation patterns and synoptic conditions.

By enhancing our understanding of dust storm mechanisms in this region, we can better mitigate their environmental and health impacts on affected populations

5. Conclusion

In recent years, the increased frequency of dust storms has attracted researchers' attention to this phenomenon, resulting in significant progress in international studies. Their research areas include: dust detection using various indices on different satellite images and evaluating their quality, identifying the source and transfer paths of dust using remote sensing, and the effects of dust on human health and the environment. The frequency of their occurrence at different time scales and the reasons for their varying frequencies are studied using precise methods. In domestic sources, significant progress has also been made in this field compared to before. These studies

focus more on the synoptic causes of frequent storms and the trend of dusty days in smaller areas. [19]

The research findings in the synoptic section lead us to the conclusion that by jointly analyzing remote sensing data and weather maps, we can conclude that to model, study, and predict dust movement, it is necessary to examine weather maps of geopotential height at 500 mb pressure (HGT) and wind flow direction maps at 500 and 1000 mb levels. This means that both surface and upper-atmosphere maps should be examined simultaneously, and one cannot reach an appropriate conclusion by examining only one of the weather maps. [20]

Considering the studies conducted and the research findings in the remote sensing section, the results are as follows: In tracing the origin of dust particles in the studied storm, the source of dust phenomena entering western, southern, and southwestern Iran is in Syria. It is clear that the initial point of dust uplift contains fine river sediments. These areas were previously swampy and have become dry basins due to unusual water use upstream of rivers in Syria. Human activities in these areas have expanded the dust activity basin. Therefore, with the destruction of the region's vegetation cover, fine soil particles are displaced by winds, creating dust storms. [21,26]

Acknowledgement

I would like to express my gratitude to NASA for providing access to satellite images that significantly contributed to the research conducted in this study. The availability of these images enabled a comprehensive analysis of dust phenomena, allowing for improved understanding and insights into the dynamics of dust storms. This support is invaluable for advancing scientific research and enhancing our knowledge of environmental changes. Thank you, NASA, for your commitment to facilitating research through the provision of essential data resources.

Author contributions

Ali Ibrahim Zaghir: Conceptualization, Methodology, Software, Field study **Khalil Valizadeh Kamran:** Data curation, Writing-Original draft preparation, Software, Validation., Field study **Sadra Karimzadeh:** Visualization, Investigation, Writing-Reviewing and Editing.

Conflicts of interest

The authors declare no conflicts of interest.

References

1. Sivakumar, M. V. K. (2005). Impacts of sand storms and dust storms on agriculture. In M. V. K. Sivakumar, R. P. Motha, & H. P. Das (Eds.), *Natural Disasters and Extreme Events in Agriculture* (pp. 159-177). Springer. https://doi.org/10.1007/3-540-28307-2
2. Abbasi, H., Rafiei Emam, A., & Rouhi Pour, H. (1999). Analysis of the origin of dust in Bushehr and Khuzestan using satellite images. *Forest and Rangeland Quarterly*, *78*, 48-51.
3. Zolfaghari, H., & Abedzadeh, H. (2005). Synoptic analysis of dust storms in western Iran. *Journal of Geography and Development*, *6*, 27.
4. Raeispour, K. (2008). Statistical and synoptic analysis of dust phenomenon in Khuzestan (Master's thesis, Climatology in Environmental Planning, University of Sistan and Baluchestan), p. 157.
5. Maghrabi, A., Alharbi, B., & Tapper, N. (2011). Impact of the March 2009 dust event in Saudi Arabia on aerosol optical properties, meteorological parameters, sky temperature and emissivity. *Atmospheric Environment*, *45*(12), 2164-2173. https://doi.org/10.1016/j.atmosenv.2011.01.018
6. Mie, D., Xiushan, L., Lin, S., & Ping, W. (2008). A dust-storm process dynamic monitoring with multi-temporal MODIS data. In *the International Archives of Photogrammetry, Remote Sensing and Spatial Information Sciences* (Vol. XXXVII, Part B7, pp. 965–969). https://doi.org/10.5194/isprsarchives-XXXVII-B7-965-2008
7. Tsolmon, R., Ochirkhuyag, L., & Sternberg, T. (2008). Monitoring the source of transnational dust storms in North East Asia. *International Journal of Digital Earth*, *1*, 119-129. https://doi.org/10.1080/17538940701782593
8. Solomos, S., Ansmann, A., Mamouri, R.-E., Binietoglou, I., Patlakas, P., Marinou, E., & Amiridis, V. (2017). Remote sensing and modelling analysis of the extreme dust storm hitting the Middle East and eastern Mediterranean in September 2015. *Atmospheric Chemistry and Physics*, *17*, 4063–4079. https://doi.org/10.5194/acp-17-4063-2017
9. Darvishi, B. A., Kazemi, Y., Sadeghi, A., Nadizadeh, S. S., & Argany, M. (2020). Identification of dust sources using long term satellite and climatic data: A case study of Tigris and Euphrates basin. *Environmental Pollution*, *263*, 114404. https://doi.org/10.1016/j.envpol.2020.114404
10. Darvishi Boloorani, A., Papi, R., Soleimani, M., Al-Hemoud, A., Amiri, F., Karami, L., Neysani, S. N., Bakhtiari, M., & Mirzaei, S. (2023). Visual interpretation of satellite imagery for hotspot dust sources identification. *Computers in Earth Sciences*, *235*, 1963. https://doi.org/10.1016/j.cgs.2022.1963
11. NASA Earth Observatory. (2007). Dust storm over Syria, Turkey, and Iraq. Retrieved from https://earthobservatory.nasa.gov/images/18388/dust-storm-over-syria-turkey-and-iraq
12. ResearchGate. (n.d.). Satellite image of dust storm: a) Composite map of pressure and wind vector at 850 hPa. Retrieved from https://www.researchgate.net/figure/Satellite-image-of-dust-storm-a-b-composite-map-of-pressure-and-wind-vector-at-850hPa_fig3_350008218
13. Valizadeh Kamran, K. and Khorrami, B.: Change Detection and Prediction of Urmia Lake and its Surrounding Environment During the Past 60 Years Applying Geobased Remote Sensing Analysis, Int. Arch. Photogramm. Remote Sens. Spatial Inf. Sci., XLII-3/W4, 519–525, https://doi.org/10.5194/isprs-archives-XLII-3-W4-519-2018, 2018.

14. Nasir, S. M., Kamran, K. V., Blaschke, T., & Karimzadeh, S. (2022). Change of land use/land cover in kurdistan region of Iraq: A semi-automated object-based approach. *Remote Sensing Applications: Society and Environment*, *26*, 100713. https://doi.org/10.1016/j.rsase.2022.100713
15. Rezaeimoghadam, M., Valizadeh Kamran, K., Rostamzadeh, H., & Rezaee, A. (2013). Evaluating the Adequacy of MODIS in the Assessment of Drought (Case Study: Urmia Lake Basin). *Geography and Environmental Sustainability*, *2*(4), 37-52.
16. Çörek Öztaş, Ç., & Karaaslan, Ş. (2018). Coğrafi Bilgi Sistemleri (CBS) İle İlçeler Düzeyinde Kırsallık Kademelerinin Hazırlanmasına Yönelik Bir Yöntem Önerisi. Geomatik, 3(2), 163-182. https://doi.org/10.29128/geomatik.376253
17. Gündüz, M. (2025). Kilistra ignimbiritlerinin uzaktan algılama yöntemleriyle yeniden haritalanması ve Beyşehir Havzası'nın (GB Konya/Türkiye) CBS tabanlı çizgisellik analizi. Geomatik, 10(1), 76-91. https://doi.org/10.29128/geomatik.1533893
18. Patil, R., & Datta , M. . (2022). Spatio-Temporal Analysis of Climate Change in India: a Theoretical Perspective. *Advanced Geomatics*, *2*(1), 07–13. Retrieved from https://publish.mersin.edu.tr/index.php/geomatics/article/view/168
19. Tabakoğlu, C. (2024). A Review: Detection types and systems in remote sensing. *Advanced GIS*, *4*(2), 100–105. Retrieved from https://publish.mersin.edu.tr/index.php/agis/article/view/1560.
20. Zeynalov, I., Akhmedova , R. ., Akhmedova , A. ., & Rustamova , A. . (2024). Analysis of the sea surface temperature (SST) of the Caspian Sea from NOAA satellites. *Advanced Remote Sensing*, *4*(1), 1–10. Retrieved from https://publish.mersin.edu.tr/index.php/arsej/article/view/1164
21. Tahsin, A. ., Abdullahi, J. ., Karabulut, A. İzzeddin, & Yesilnacar, M. I. . (2023). Spatiotemporal prediction of reference evapotranspiration in Araban Region, Türkiye: A machine learning based approach. *Advanced Remote Sensing*, *3*(1), 27–37. Retrieved from https://publish.mersin.edu.tr/index.php/arsej/article/view/833
22. Boutallaka, M., Miloud, T., El Mazi, M., Hmamouchi, M., et al. (2025). Assessment of current and future land sensitivity to degradation under climate change in the upstream Ouergha watershed (Morocco) using GIS and AHP method. International Journal of Engineering and Geosciences, 10(1), 46-58. https://doi.org/10.26833/ijeg.1521350
23. Yılmaz, V. (2025). Climate patterns in Europe: A focus on ten countries through remote sensing. International Journal of Engineering and Geosciences, 10(3), 398-418. https://doi.org/10.26833/ijeg.1583206
24. Yaman, Ş., & Yaman, M. (2024). Creation of Turkiye risk map for Cydalima perspectalis (box tree moth) by weighted overlay analysis. International Journal of Engineering and Geosciences, 9(3), 345-355. https://doi.org/10.26833/ijeg.1434437
25. Ünel, F. B., Kuşak, L., Yakar, M., & Doğan, H. (2023). Coğrafi bilgi sistemleri ve analitik hiyerarşi prosesi kullanarak Mersin ilinde otomatik meteoroloji gözlem istasyonu yer seçimi. *Geomatik*, *8*(2), 107-123.
26. Yilmaz, H. M., Yakar, M., Mutluoglu, O., Kavurmaci, M. M., & Yurt, K. (2012). Monitoring of soil erosion in Cappadocia region (Selime-Aksaray-Turkey). *Environmental Earth Sciences*, *66*, 75-81.